HAL
open science

Confocal thermal-lens microscope

Julien Moreau, V. Loriette

To cite this version:

Julien Moreau, V. Loriette. Confocal thermal-lens microscope. Optics Letters, 2004, 29 (13), pp.1488. 10.1364/OL.29.001488 . hal-00624810

HAL Id: hal-00624810

https://hal.science/hal-00624810v1

Submitted on 19 Sep 2011

HAL is a multi-disciplinary open access archive for the deposit and dissemination of scientific research documents, whether they are published or not. The documents may come from teaching and research institutions in France or abroad, or from public or private research centers.

L'archive ouverte pluridisciplinaire **HAL**, est destinée au dépôt et à la diffusion de documents scientifiques de niveau recherche, publiés ou non, émanant des établissements d'enseignement et de recherche français ou étrangers, des laboratoires publics ou privés.

Confocal thermal-lens microscope

Julien Moreau and Vincent Loriette

Centre National de la Recherche Scientifique, Unité Propre de Recherche 5, École Supérieure de Physique et Chimie Industrielles de la Ville de Paris, Laboratorie d'Optique Physique, 10 Rue Vauquelin, 75005 Paris, France

Received October 24, 2003

The use of a confocal detection scheme in a dual-beam thermal-lens microscope is presented. The scheme allows the measurement of absorption factors down to 1.2×10^{-7} in a 0.35-μm^3 volume by use of a heating laser power of 100 mW incident upon the sample. Results are presented that prove that a 450-nm axial resolution is possible when a 1.2 water immersion objective lens with a N.A. of 1.2 is used. © 2004 Optical Society of America

OCIS codes: 180.1790, 350.6830.

Thermal lensing provides high-sensitivity measurements for thermal[1] and spectroscopic[2] characterization or detection[3–5] and imaging[6] of low-absorption samples. Thermal-lens microscopy[7] combines the high sensitivity of photothermal techniques[8] with the lateral and axial resolution of conventional microscopy. The detection method used in thermal-lens microscopy does not differ from conventional thermal-lens techniques[9]: The thermal lens generated by a heating beam induces a change in the geometric parameters (divergence and beam-waist position) of a probe beam that are detected with the help of a diaphragm placed in the path of the beam in front of a photodetector. With this detection method the signal is maximum when the thermal lens is located at a distance of one heating beam's Rayleigh range from the probe beam's waist; it is null when the thermal lens lies in the plane of the probe beam's waist.[7] The axial resolution (FWHM) of the thermal lens microscope is given by the following formula:

$$\Delta z_{\text{standard}} \approx 2.8 \times z_R \,, \tag{1}$$

where z_R is the heating beam's Rayleigh range at the focal point. Thermal lens microscope signals exhibit two main drawbacks when one needs to resolve structures in the axial direction. First, the signal's shape (see Fig. 1), which shows two extrema that correspond to focusing or defocusing by the thermal lens, and a zero point crossing make it difficult to use efficient deconvolution algorithms. Second, it can be shown that the relative height of the two extrema strongly depends on the distance between the two beam waists, and it is quite difficult to control that parameter, which depends on the beams' different geometric parameters and on the chromatic characteristics[7] of the microscope objective lens that is used. Our detection scheme aims at eliminating these two drawbacks. The thermal lens microscope is not an imaging, but a scanning, instrument, so a detection scheme similar to confocal microscopy can be used. The axial resolution can then be improved to

$$\Delta z_{\text{confocal}} \approx 1.0 \times z_R \,. \tag{2}$$

In this case the signal is now maximum when the thermal lens lies in the plane of the probe beam's waist and so exhibits only one extremum (see Fig. 1). This increase of resolution and the single maximum signal shape can be used to study transparent stratified samples such as dielectric multilayer coatings. It permits discrimination of the photothermal signal generated by the different layers and possibly by the different interfaces. It is worth noting that this significant increase of axial resolution is not obtained to the detriment of sensitivity. It can be shown, on the contrary, that a signal increase of a factor 2 can be obtained at the same time. Figure 1 illustrates this point by comparing calculations of classical and confocal thermal-lens signals performed in the paraxial approximation (i.e., by considering Gaussian beam propagation in the microscope). Another interesting feature of the confocal scheme is that, unlike in the nonconfocal case, the signal's shape is nearly insensitive to the amount of chromatic aberration caused by the focusing objective lens.

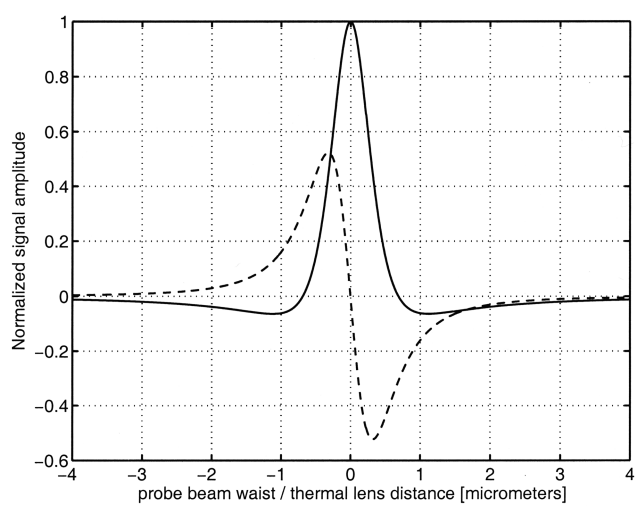

Fig. 1. Theoretical calculations of the confocal (solid curve) and the nonconfocal (dashed curve) thermal-lens signals for surface absorption. The parameters used in the calculations were $\lambda_{\text{probe}} = 638$ nm for the probe beam and $\lambda_{\text{heat}} = 514$ nm for the pump beam, a N.A. of 1.2 for the objective lens, index of refraction $n = 1.33$ for the immersion medium.

0146-9592/04/131488-03$15.00/0 © 2004 Optical Society of America

Figure 2 shows our confocal dual-beam thermal-lens microscope. The heating beam is an intensity-modulated $\lambda = 514$ nm argon laser, and the probe beam is a 1-mW unmodulated red laser diode emitting at 638 nm. The heating power is limited to 100 mW to prevent damaging the sample. The modulation frequency of 1 MHz was chosen such that the thermal diffusion length in the sample is smaller than the heating beam's spot size. Both beams pass through a beam expander before entering the focusing objective lens. After crossing the sample, the beams are collected by a second objective lens. The sample is fixed on a motorized stage that permits axial displacements in 74-nm steps. The sample is the only moving part of the experiment, so, except for geometric modifications of the beam parameters induced by aberrations caused by the sample, both beams' characteristics, in particular their beam-waist positions, do not change during scanning. After crossing the sample, the heating beam is then directed into a light trap while the probe beam passes through a pinhole and then goes onto a silicon photodetector. Pinhole diameter r_D is chosen to give the best shot-noise-limited signal-to-noise ratio; its theoretical value is

$$r_D \approx 0.57 \times w_D\,, \tag{3}$$

where w_D is the probe beam's radius on the pinhole plane. The position of the pinhole is fixed by the condition

$$z_1 + \frac{z_2}{1 - (z_2/f)} = z_{R0}\,, \tag{4}$$

where z_1 is the distance from the probe beam's waist in the sample to the imaging objective lens, z_2 is the objective lens–pinhole distance, and z_{R0} is the probe beam's Rayleigh range in the sample. This condition states that the pinhole plane is conjugate not with the plane of the probe beam's waist but with a plane that is one Rayleigh range away. One can understand why this arrangement is the correct one by looking at the effect of a lens of focal length f with $f \gg z_{R0}$ placed at the probe beam's waist (for typical values take $z_{R0} = 1\ \mu$m, and, for low-absorption samples, $f = 1$ m). In the paraxial approximation, the presence of this lens changes the beam's spot size w at a distance z after the lens by an amount equal to

$$\frac{\delta w}{w}(z) = \frac{\left[\left(1 - \frac{z}{f}\right)^2 + \frac{z^2}{{z_{R0}}^2}\right]^{1/2} - \left(1 + \frac{z^2}{{z_{R0}}^2}\right)^{1/2}}{\left(1 + \frac{z^2}{{z_{R0}}^2}\right)^{1/2}}\,. \tag{5}$$

In the confocal case one can look at a plane where $\delta w/w$ is an extremum; this happens when $z = z_{R0}$, whatever the sign of f. In this case Eq. (5) gives

$$\frac{\delta w}{w} \approx \frac{z_{R0}}{f}\,. \tag{6}$$

The signal is null when $z = 0$. This condition differs from that of conventional confocal microscopy in which the pinhole plane is conjugate with the object plane. Fulfillment of this condition is critical because it fixes the confocal behavior of the instrument. One can in practice maintain the confocality condition only by limiting z scans to a few tens of micrometers and by using identical focusing and imaging objectives. With these restrictions, few-millimeter-thick optical samples, for example, structured thin-film coatings upon transparent substrates, can be investigated. The axial resolution was measured by use of a test sample made from a single 180-nm-thick tantalum pentoxide layer deposited by ion-beam sputtering onto a synthetic fused-silica sample. The extinction and

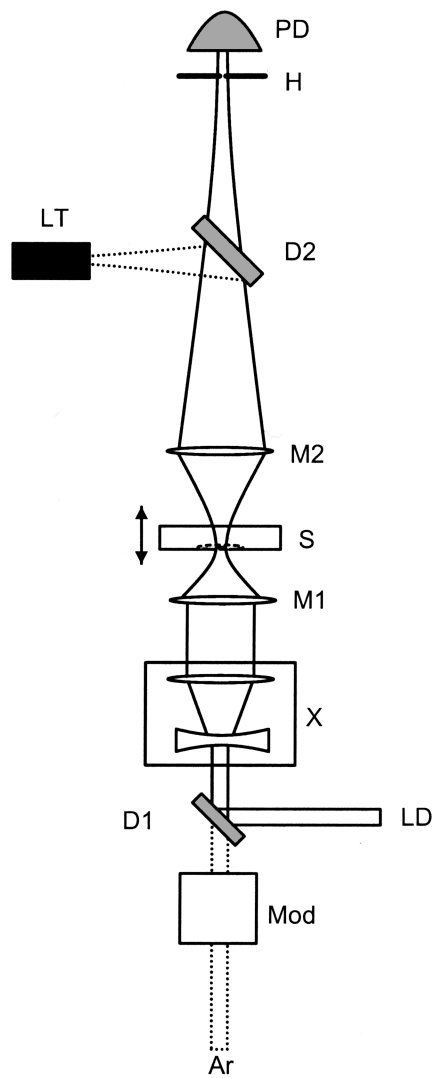

Fig. 2. Schematic of the confocal thermal-lens microscope. The heating beam is an argon laser (Ar), 100 mW of which is focused into the sample (S). Its intensity is modulated with an electro-optic modulator (Mod). The probe laser (LD) is a 1-mW 638-nm laser diode. Before entering the microscope, both beams pass through a 5× beam expander (X). M1, M2, focusing and collecting objective lenses; D1, D2, dichroic mirrors used to direct the Ar beam into a beam stop (LT) and the probe beam through a calibrated pinhole (H) and onto a photodetector (PD). We performed axial scans by moving the sample.

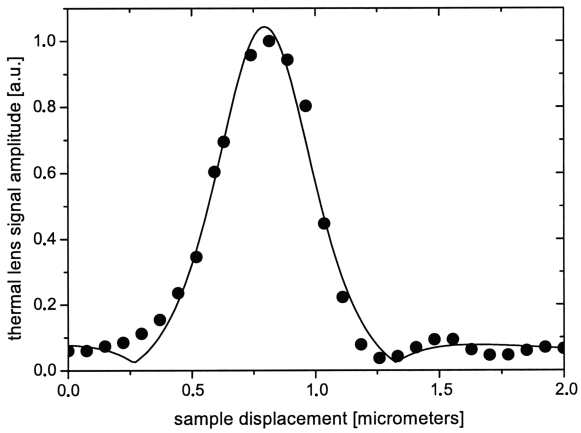

Fig. 3. Experimental confocal surface absorption signal amplitude and model. The sample is a single layer of 180-nm-thick Ta_2O_5 sputtered onto a fused-silica substrate. The layer's absorption factor was estimated to be 1.8×10^{-6}. The 900-nm resolution was achieved with a water immersion objective of 1.2 N.A.

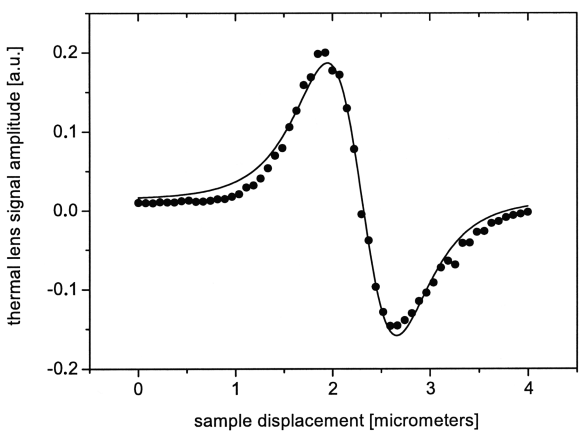

Fig. 4. Nonconfocal surface absorption signal amplitude measured with the same optical arrangement and on the same sample as in Fig. 3; the model was used.

refraction indices of the sputtered layer were measured with an ellipsometer, and the resultant absorption coefficient was found to be $\alpha \approx 10\ \mathrm{m}^{-1}$ at the argon laser wavelength. The integrated absorption factor of the layer is thus 1.8×10^{-6}.

Figure 3 shows the result of this measurement. The focusing objective lens was a water immersion lens with a N.A. of 1.2. (Olympus Model UPLanApo ×60). The experimental signal's FWHM was $\Delta z(\mathrm{exp}) = 450$ nm. Using a mathematical model of the instrument, we calculated that the confocal signal's FWHM with this objective lens should be $\Delta z(\mathrm{theoretical}) = 465$ nm. We checked the expected gain in axial resolution by moving the pinhole a few millimeters and performing the same measurement with a nonconfocal configuration. The result is presented in Fig. 4. The measured FWHM is $\Delta z(\mathrm{nonconfocal}) = 1.5\ \mu\mathrm{m}$. We then estimated the instrument's sensitivity by measuring volume absorption in a neutral-density filter with an $\alpha = 255\ \mathrm{m}^{-1}$ absorption coefficient. The fraction of absorbed power that gives rise to a thermal lens is roughly

$$P_{\mathrm{abs}}/P_p \approx \alpha \Delta z\,, \tag{7}$$

where P_p is the incident heating power. With the 1.2-N.A. objective lens we have $\alpha \Delta z = 2.1 \times 10^{-4}$. We measured a signal-to-noise ratio of 1830 when we integrated the signal for 1 s, so the smallest detectable absorption factor is estimated to be 1.15×10^{-7}.

V. Loriette's e-mail address is loriette@opitque.espci.fr.

References

1. Z. L. Wu, P. K. Kuo, Y. S. Lu, S. T. Gu, and R. Krupka, Thin Solid Films **290–291,** 271 (1996).
2. S. Kawasaki, R. J. Lane, and C. L. Tang, Appl. Opt. **33,** 992 (1994).
3. M. Tokeshi, M. Uchida, K. Uchiyama, T. Sawada, and T. Kitamori, J. Lumin. **83–84,** 261 (1999).
4. K. Mawatari, T. Kitamori, and T. Sawada, Anal. Chem. **70,** 5037 (1998).
5. M. Harada, K. Iwamoto, T. Kitamori, and T. Sawada, Anal. Chem. **65,** 2938 (1993).
6. H. Kimura, K. Sekiguchi, T. Kitamori, T. Sawada, and M. Mukaida, Anal. Chem. **73,** 4333 (2001).
7. K. Ushiyama, A. Hibara, H. Kimura, T. Sawada, and T. Kitamori, Jpn. J. Appl. Phys. **39,** Part 1, 5316 (2000).
8. S. E. Bialkowski, *Photothermal Spectroscopy Methods for Chemical Analysis* (Wiley, New York, 1996).
9. M. Franko and C. D. Tran, Rev. Sci. Instrum. **67,** 1 (1996).